Optical Engineering

OpticalEngineering.SPIEDigitalLibrary.org

# Swing arm profilometer: high accuracy testing for large reaction-bonded silicon carbide optics with a capacitive probe

Ling Xiong
Xiao Luo
Hai-xiang Hu
Zhi-yu Zhang
Feng Zhang
Li-gong Zheng
Xue-jun Zhang

SPIE.

Ling Xiong, Xiao Luo, Hai-xiang Hu, Zhi-yu Zhang, Feng Zhang, Li-gong Zheng, Xue-jun Zhang, "Swing arm profilometer: high accuracy testing for large reaction-bonded silicon carbide optics with a capacitive probe," *Opt. Eng.* **56**(8), 084101 (2017), doi: 10.1117/1.OE.56.8.084101.

# Swing arm profilometer: high accuracy testing for large reaction-bonded silicon carbide optics with a capacitive probe

**Ling Xiong,[a,b] Xiao Luo,[a] Hai-xiang Hu,[a,b] Zhi-yu Zhang,[a] Feng Zhang,[a] Li-gong Zheng,[a,*] and Xue-jun Zhang[a]**
[a]Changchun Institute of Optics, Fine Mechanics and Physics, Key Laboratory of Optical System Advanced Manufacturing Technology, Chinese Academy of Sciences, Changchun, China
[b]University of Chinese Academy of Sciences, Beijing, China

**Abstract.** A feasible way to improve the manufacturing efficiency of large reaction-bonded silicon carbide optics is to increase the processing accuracy in the ground stage before polishing, which requires high accuracy metrology. A swing arm profilometer (SAP) has been used to measure large optics during the ground stage. A method has been developed for improving the measurement accuracy of SAP using a capacitive probe and implementing calibrations. The experimental result compared with the interferometer test shows the accuracy of 0.068 $\mu$m in root-mean-square (RMS) and maps in 37 low-order Zernike terms show accuracy of 0.048 $\mu$m RMS, which shows a powerful capability to provide a major input in high-precision grinding.  [DOI: 10.1117/1.OE.56.8.084101]

Keywords: surface test; profilometer; calibration; ground phase.

Paper 170064 received Jan. 12, 2017; accepted for publication Jun. 7, 2017; published online Aug. 4, 2017.

## 1 Introduction

Optics with large apertures provide high-angular resolution and powerful energy-gathering ability. They are now widely used in astronomical observation and earth observation systems. Considering their excellent thermostability, specific stiffness, etc., silicon carbide (SiC) material has been selected in more and more optic systems. Fabrication of large optical surfaces is difficult because of the complicated tooling needed for all stages of manufacturing and measuring. It is especially difficult for fabricating SiC surfaces, because this kind of material is so hard to remove. The general fabrication process of large optical surfaces includes milling, grinding, and polishing. For SiC mirrors, the material removal rate of polishing is much lower than that of grinding. To achieve a high efficiency of overall fabrication, it is good to remove as much surface residue as possible during the grinding process. Thus, a more precise measurement is needed as an input.

A swing arm profilometer (SAP) was first reported by Anderson et al. from the University of Arizona and has been used for measuring large aspheric optics with an excellent performance rivaling full aperture interferometric tests for accuracy of 5-nm root-mean-square (RMS) with the 43 low-order Zernike terms removed during the polishing process.[1–4] In recent years, the Arizona group has developed SAP to test ground aspheric surfaces with a laser triangulation probe to a precision better than 0.1-nm RMS with astigmatism, coma, and trefoil removed.[5] Groups from London and Chengdu China have also done a lot of good work on SAP testing; the measurement uncertainty of the prototype SAP was reported to be 2.4 $\mu$m in peak-valley (PV) and 0.5 $\mu$m in RMS.[6–8] The accuracy of other works from South Korea[9] or Changsha China[10] was reported to be microns in PV. The techniques of the SAP test from Changchun Institute of Optics, Fine Mechanics and Physics have allowed successful measurement to an accuracy of 0.087 $\mu$m in RMS for the 37 low-order Zernike terms.[11] Our goal is to achieve a higher accuracy of SAP for SiC mirrors during the grinding process.

Recently, we developed an enhanced SAP equipped with an ultraprocess capacitive sensor to measure the electric conductive reaction-bonded silicon carbide (RB-SiC) optics. Compared with the laser displacement sensors, the capacitive displacement sensor achieves higher resolution at the subnanometer level with better stability. In this paper, first the basic principle of the SAP test and capacitive sensor is simply introduced in Sec. 2. Then to ensure the accuracy of the capacitive sensor, we implemented the experimental calibration on an ultraprecise single point diamond turning (SPDT) machine as presented in Sec. 3. There, the dynamic stability about temperature and the linearity of the capacitive probe was tested, and error induced from the tilt factor between the target and probe was discussed. Finally with those calibrations, an experimental test with SAP was performed to measure an $1100 \times 800$ mm RB-SiC mirror as described in Sec. 4.

## 2 Principles

### 2.1 *Principle of SAP*

SAP is developed to measure aspheric surfaces with respect to a sphere reference instead of a traditional plane reference such as a coordinate measuring machine. In measuring the deviation from the best-fit sphere (BFS), a higher accuracy sensor with shorter range can be selected.

The basic geometry of the SAP is shown in Fig. 1(a), a probe is mounted at the end of an arm that is fixed on a high

*Address all correspondence to: Li-gong Zheng, E-mail: zhenglg@ciomp.ac.cn

0091-3286/2017/$25.00 © 2017 SPIE

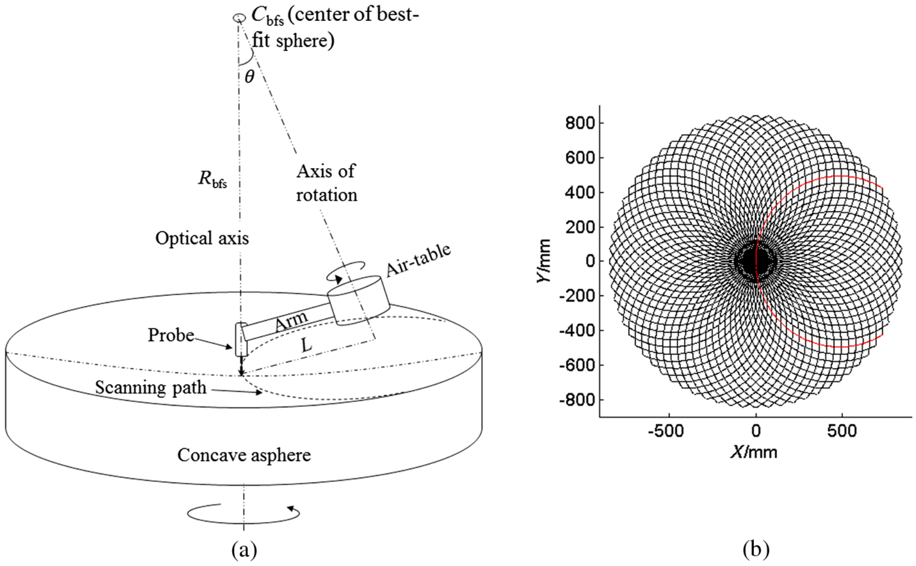


**Fig. 1** Basic principle of SAP test: (a) geometry of SAP and (b) scan pattern.

accuracy air-table whose rotation axis is tilted and goes through the center of BFS. By rotating the mirror, a two-dimensional profile can be obtained with multiple scans as shown in Fig. 1(b). The tilt-angle $\theta$ of air-table is given as

$$\theta = \sin^{-1}\left(\frac{L}{R_{\mathrm{bfs}}}\right), \tag{1}$$

where $L$ is the distance between probe tip and rotation axis of air-table and $R_{\mathrm{bfs}}$ is the radius of curvature of BFS. The surface error is given by $\Delta S = S_t - S_0$, where $S_t$ is the probe reading and $S_0$ is the ideal aspherical departure from the BFS.[12,13]

### 2.2 *Principle of Capacitive Displacement Sensor*

A capacitive displacement sensor is based on principle of testing the reactance of the plate capacitor. As shown in Fig. 2, the sensor and the conductive target opposite form the two plate electrodes. If an AC current with a constant amplitude flows through the sensor capacitor, the amplitude of the AC voltage at the sensor is proportional to the distance between the capacitor electrodes. The reactance $X_c$ of the plate capacitor that changes strictly in proportion to the distance[14]

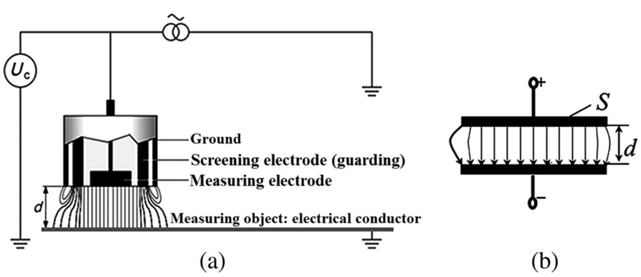


**Fig. 2** (a) Structure of a capacitive sensor and (b) principle of a plate capacitor.

$$X_c = \frac{1}{j \cdot \omega \cdot C}, \tag{2}$$

$$\text{Capacitance}: C = \varepsilon_{\mathrm{r}} \cdot \varepsilon_0 \cdot \frac{S}{d}, \tag{3}$$

where $\varepsilon_{\mathrm{r}}$ and $\varepsilon_0$ are vacuum permittivity and relative permittivity, respectively; $S$ is the area of plate and $d$ is the distance between two plates.

## 3 Calibrations

In this paper, with the ultraresolution capacitive sensor, our goal aims to achieve the accuracy of the SAP test to better than 0.1-$\mu$m RMS in the overall shape and 0.5-$\mu$m PV, 0.05-$\mu$m RMS in low-order (first 37 Zernike terms).

The parameters of the capacitive sensor are listed in Table 1. Although it has excellent resolution and stability, it has some disadvantages for application. One is that the sensor plate needs to be aligned parallel to the target plate. Another is that the capacitive sensor may be sensitive to temperature variation. Moreover, the nominal linearity is 0.5 $\mu$m, which also needs to be calibrated for higher accuracy.

To improve the accuracy of the capacitive sensor, we implemented the experimental calibration on an SPDT machine shown in Fig. 3. The positioning accuracy of the

**Table 1** Parameters of a 1-mm sensor.

| Item | Parameters |
|---|---|
| Measurement range | 1 mm |
| Nominal linearity | 0.5 $\mu$m |
| Resolution | 0.75 nm |
| Diameter of outer cylinder | Ø10 mm |
| Active measuring area | Ø5.7 mm |

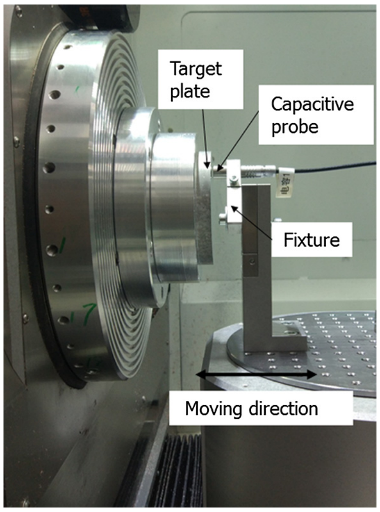


**Fig. 3** Experimental setup for sensor calibration on SPDT machine.

**Table 2** Calibration budget.

| Calibration items | Accuracy |
|---|---|
| Thermal | 0.1 $\mu$m |
| Linearity | 0.1 $\mu$m |
| Tilt | 0.1 $\mu$m |

SPDT machine in the moving direction was 8 nm. The measurement target was an aluminum plane mirror with flatness less than 0.05 $\mu$m. First, the dynamic stability of the temperature and the linearity of the capacitive probe were tested using the SPDT machine.

Then error induced from the tilt factor between the target and probe was discussed. We had formulated a budget for each calibration shown in Table 2, to achieve an ability of 0.3-$\mu$m PV for low-order terms.

### 3.1 *Dynamic Stability*

The probe was fixed on the axes of the SPDT machine in front of the mirror. The distance between the probe and the mirror was 500 $\mu$m in the middle value of the measuring range. To check the temperature variation characteristic of the capacitive probe, a large number of long-time measurements were carried out. During a 12-h detection, temperature drift from 28.5°C to 25.2°C and probe reading changed from 499.8 $\mu$m to 501.5 $\mu$m. It can be seen from Fig. 4 that the change of rate was $-0.7$ $\mu$m/°C. Sampling frequency for the sensor was 2.8 Hz and for the temperature was 0.1 Hz. During the SAP test mentioned later in this paper, it would take about 30 s for a single scan, where the temperature variation was less than 0.1°C. So the errors induced from temperature variation would be within 0.07 $\mu$m.

### 3.2 *Linearity Deviation*

To check its linearity deviation, the sensor was carried to go along the moving direction shown in Fig. 3 by a step of 10 $\mu$m. The route was in the range of 1000 $\mu$m and it was paused 5 s at each step. The sampling frequency of the sensor was set to be 10 Hz. Probe readout in a single measurement was displayed in Fig. 5. Six data sets were collected counting back and forth in the route.

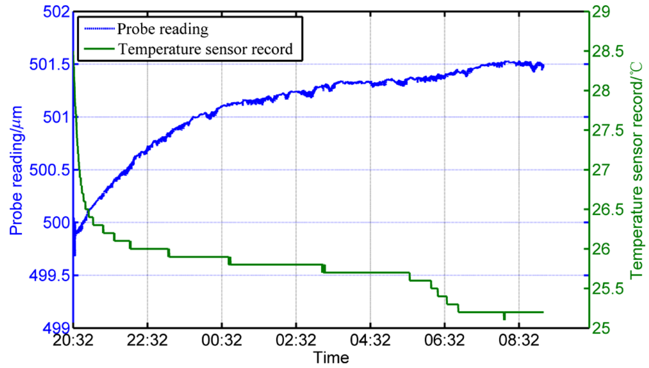


**Fig. 4** Record of probe reading and the temperature during 12 h.

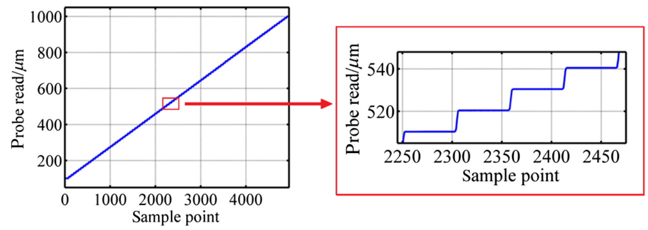


**Fig. 5** Single measurement of raw data.

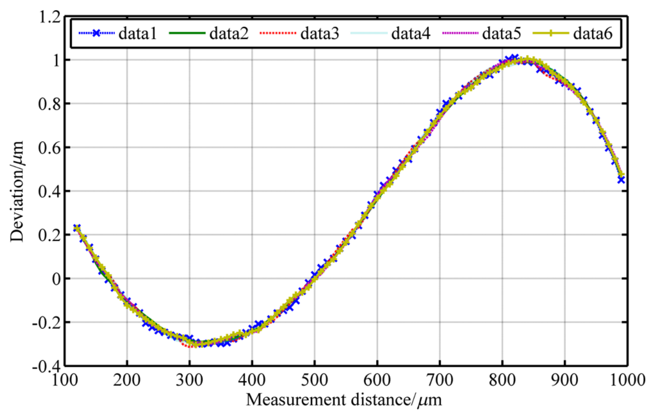


**Fig. 6** Six sets of linearity deviation for sensor calibration.

The linearity deviations for six data sets were 1.3 in 1000 $\mu$m range shown in Fig. 6. Because of vibration and noise, the uncertainty of the calibration data was 0.01 $\mu$m (in a sigma). The uncertainty of the calibration was defined by the difference between each set of data and the average value, as shown in Fig. 7.

### 3.3 *Tilt Factor*

For a perfect measurement, the target plane and the probe plane are supposed to be paralleled, while in a practical situation, it may not be possible. The measurement error induced from two unparalleled palates is discussed below. As shown in Fig. 8, the capacitance between two plates that are relatively tilted by $\theta$ is given as

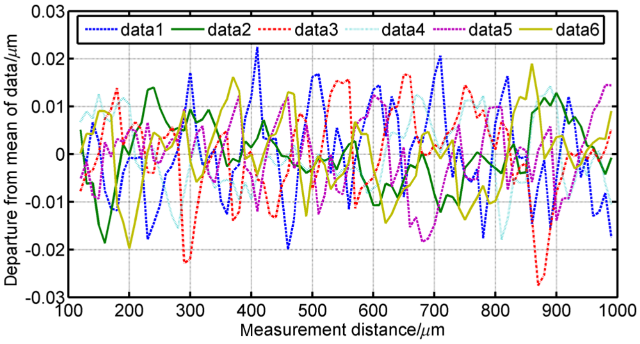


**Fig. 7** Departure of each set from mean of data set.

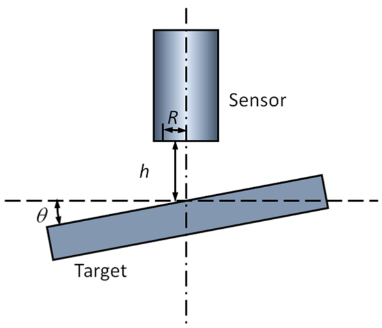


**Fig. 8** Diagrammatic drawing for target unparallel to sensor.

$$C = \varepsilon_0 \varepsilon_r \int_0^R \rho d\rho \int_0^{2\pi} \frac{d\alpha}{h + \rho \cos \alpha \tan \theta}, \tag{4}$$

where $h > (\rho \tan \theta)^2$. The probe readout can be derived as

$$h_{\text{read}} = \frac{h}{2} \left[ 1 + \sqrt{1 - \left( \frac{R \tan \theta}{h} \right)^2} \right], \tag{5}$$

where $h$ is the distance between center of the probe plate and target plate and $R$ is the diameter of the active measurement area.

According to Eq. (5), the differences between the probe readout and center distance were displayed in Fig. 9, where targets relatively tilted by 0.1 deg, 0.2 deg, and 0.5 deg, respectively, and test distances ranged from 200 to 1000 $\mu$m. It is known from the curves that, as center distance increases, the induced error decreases. So, a far displacement measurement applied for SAP is suggested. For example, if the measuring range is within 100 $\mu$m, the capacitive probe is suggested to be mounted with a reading range from 900 to 1000 $\mu$m.

In the surface measurement mentioned later in this paper, the sensor was adjusted to the test range from 500 to 600 $\mu$m shown as the two yellow vertical lines in Fig. 9. And in that interval, the induced errors are less than 0.03 $\mu$m by 0.1-deg angle tilted, 0.12 $\mu$m by 0.2-deg angle tilted, and 0.78 $\mu$m by 0.5-deg angle tilted. As tilt angle increases, the errors induced increase rapidly. To clarify the tendency of the errors induced by different angles tilted, a curve was displayed shown in Fig. 10. Hence, in our budget of sensor tilted error of 0.1 $\mu$m listed in Table 2, the probe needs to be aligned to a tilt angle within 0.7 deg.

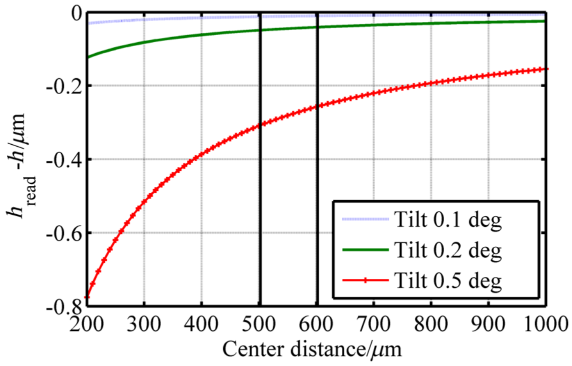


**Fig. 9** The difference between probe readout and center distance in 200 to 1000 $\mu$m range when target tilts 0.1 deg, 0.2 deg, and 0.5 deg relatively.

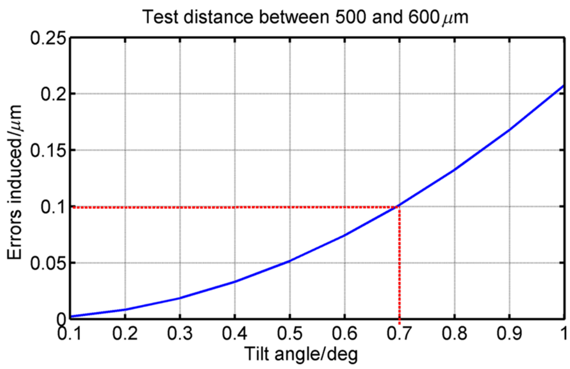


**Fig. 10** Error induced by different angles tilted in test distance between 500 and 600 $\mu$m.

In the calibration experiment, the angle of relative tilt was assembled to within 0.1 deg. In that case, it would lead to 0.035 $\mu$m errors in the overall measurement range, which coupled weakly into the calibration mentioned above and can be neglected. During the surface test mentioned later in this paper, the probe was aligned to minimize the relative tilt to a level of 0.2 deg.

## 4 Surface Measurement

With those calibrations, an experimental test with the probe equipped on SAP was performed on an $1100 \times 800$-mm spherical RB-SiC mirror. The radius of the sphere is 8870 mm. The measurement setup is shown in Fig. 11.

According to our previous work,[13] the SAP system was assembled strictly to high accuracy. The probe was seated on the center of the mirror and adjusted on the arm of the SAP to make sure that the cylinder axis of the probe was perpendicular to the surface. Papers of 10 $\mu$m thickness were inserted into the gap to check the tilt interval between the mirror and the probe. The tilt can be modified to a level of

$$\varepsilon = \frac{10\ \mu\text{m}}{D}, \tag{6}$$

where $D$ is 10 mm, the diameter of the probe. So $\varepsilon = 10^{-3}$ rad $\approx 0.06$ deg, this was within the tilt budget discussed in Sec. 3.3.

The sensor to mirror spatial coordinate was established with a commercial Laser Tracker. The related coordinate

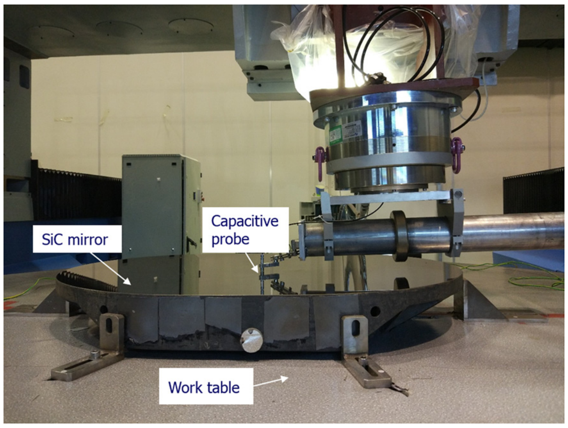


**Fig. 11** Measurement setup of SAP equipped with a capacitive probe.

system was shown in Fig. 1(a). Coordinate system $OXYZ$ and $O_2X_2Y_2Z_2$ are both in the right-hand coordinate. Since the detecting region of the capacitive probe was a circle region, the probe readout was defined as the surface departure at the center of the detecting region. The cylinder axis of the capacitive probe was tested by a commercial Laser Tracker and adjusted to the center of the mirror under test. The sensor to mirror spatial coordinate is established by measuring the tilt angle $\theta$ of the air-table and arm length $L$ shown in Fig. 1(a).

During the surface test, the mirror was scanned in 72 equal arcs. Each profile was scanned four times. The profile of a single scan ranged from 550 to 575 $\mu$m shown in Fig. 12. The trajectory of each scan arc was shown in Fig. 13.

The surface reconstitution algorithm was based on that surface heights at an intersection from two scan arcs must be the same 11 and system error can be removed according to the crossing height information. The stitched map was shown in Fig. 14. The surface test result from the SAP was 1.126-$\mu$m PV and 0.125-$\mu$m RMS.

A comparison from the interferometer test was 1.262-$\mu$m PV and 0.139-$\mu$m RMS shown in Fig. 15. Only the power item was ignored in both tests. A direct subtraction of two maps shows a difference of 0.63 $\mu$m in PV and 0.068 $\mu$m in RMS in Fig. 16.

In order to check the test precision of low-order surface errors, the 37 low-order Zernike shapes from the subtraction map were shown in Fig. 17. The precision was 0.278-$\mu$m PV

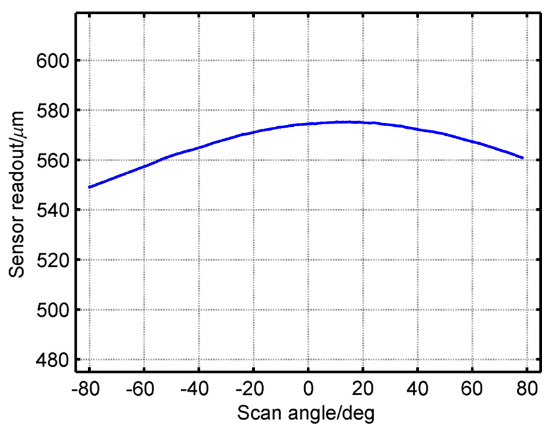


**Fig. 12** Raw data of a single scan in SAP test.

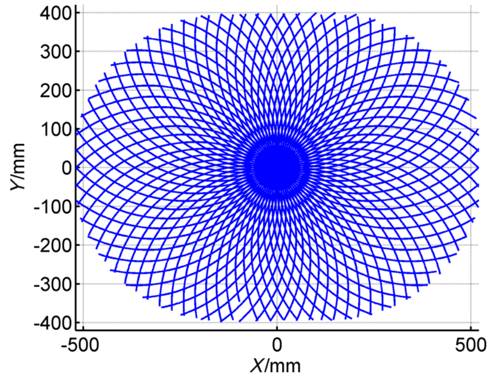


**Fig. 13** Trajectory of each scan arcs in SAP test.

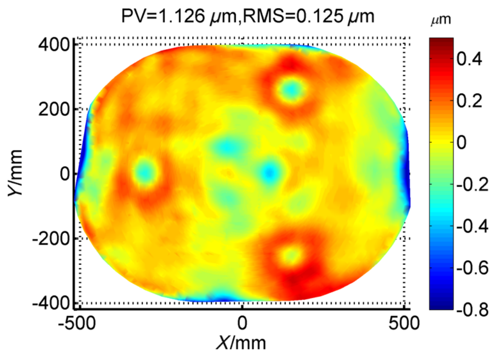


**Fig. 14** SAP test result for the mirror.

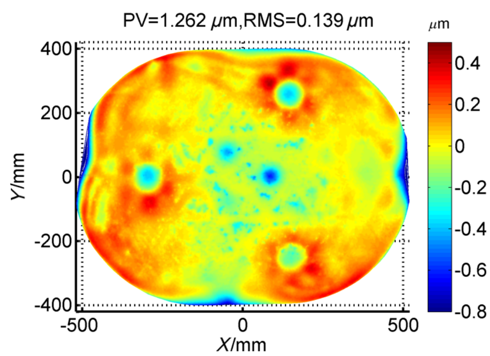


**Fig. 15** Interferometer test result for the mirror.

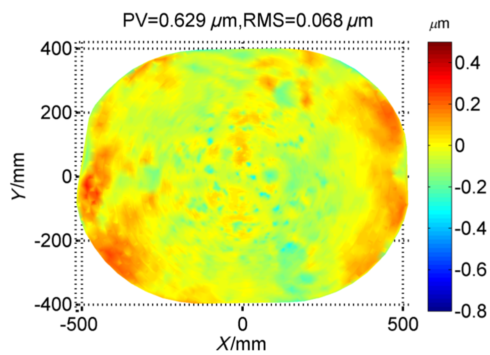


**Fig. 16** Difference between SAP and interferometer test result.

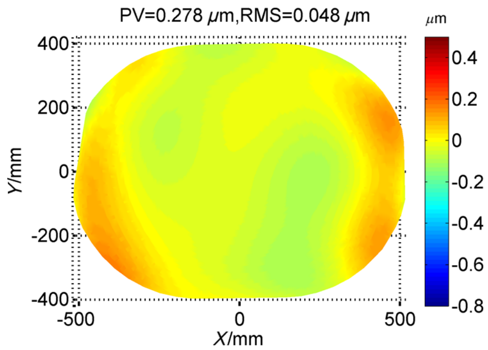


**Fig. 17** Difference between SAP and interferometer test result of 37 low-order Zernike terms.

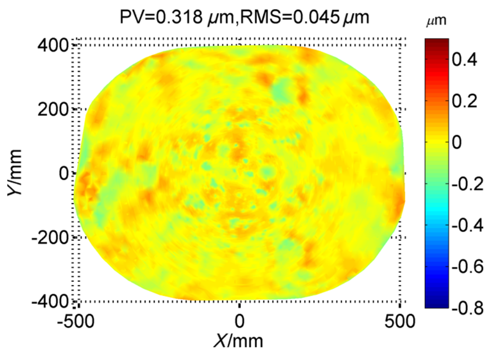


**Fig. 18** Difference between SAP and interferometer test result with 37 low-order Zernike removed.

and 0.048-$\mu$m RMS. A higher accuracy test result was achieved compared with the test result with a spectrum confocal sensor in Ref. 11, where accuracy for 37 low-order Zernike terms was 0.548-$\mu$m PV and 0.087-$\mu$m RMS. As for higher order errors shown in Fig. 18, the environmental vibration errors and errors from the air-table during the *in situ* measurement were the main source which will be studied in our future work.

## 5 Conclusion

This paper provides a guide for the ultraprecision capacitive sensor to be applied on SAP. Notice that the application is suitable only for electrical conductive optics such as the RB-SiC mirror. To achieve the goal of test accuracy of 0.5-$\mu$m PV, 0.05-$\mu$m RMS in low-order terms (first 37 Zernike terms) proposed, the calibration budget was given and a calibrating experiment proceeded on the SPDT machine. The errors induced from the temperature variation were within 0.07 $\mu$m; linearity deviation of the sensor was calibrated to within 0.05 $\mu$m; error induced from unparallel to surface are within 0.1 $\mu$m for a tilt angle within 0.7 deg. Other errors such as signal noise of the sensor, vibration errors from environment, and air-table and so on mainly resulted in high-order aberrations and was not concerned in this paper.

For measuring a $1100 \times 800$-mm spherical RB-SiC mirror, the accuracy of 0.068 $\mu$m in RMS is very encouraging. As the low-order terms of surface residue are the major part to be removed during the grinding process, the more concerning accuracy for 37 low-order Zernike items are 0.278-$\mu$m PV and 0.048-$\mu$m RMS. Compared with the SAP test with a spectrum confocal sensor in Ref. 11, where accuracy for 37 low-order Zernike terms is 0.548-$\mu$m PV and 0.087-$\mu$m RMS, the capacitive probe shows a more powerful capability for guiding higher-precision fabrication in the grinding process.

### Acknowledgments

This work was supported by the National Natural Science Foundation of China (61605202, 61210015) and the National High Technology Research and Development Program of China (O8663NJ090).

### References

1. D. S. Anderson, R. E. Parks, and T. Shao, "A versatile profilometer for aspheric optics," in *Proc. of OF&T Workshop Technical Digest*, Vol. 11, pp. 119–122, Academic, Monterrey, California (1990).
2. D. S. Anderson and J. H. Burge, "Swing-arm profilometry of aspherics," *Proc. SPIE* **2536**, 169 (1995).
3. P. Su et al., "Swing arm optical CMM for aspherics," *Proc. SPIE* **7426**, 74260J (2009).
4. J. H. Burge, "Fabrication and testing of 1.4-m convex off-axis aspheric optical surfaces," *Proc. SPIE* **7426**, 74260L (2009).
5. Y. Wang et al., "Swing arm optical coordinate-measuring machine: high precision measuring ground aspheric surfaces using a laser triangulation probe," *Opt. Eng.* **51**(7), 073606 (2012).
6. A. Lewis et al., "Accurate arm profilometry traceable metrology for large mirrors," in *Proc. of Simposio de Metrología*, pp. 101–105, Academic, Mexico (2006).
7. H. Jing et al., "Development and experimental validation of a versatile prototype swing arm profilometer for measuring optical surface," *J. Eur. Opt. Soc. Rapid Publ.* **6**, 11052 (2011).
8. H. Jing et al., "Measurement of an off-axis parabolic mirror using coordinates measurement machine and swing arm profilometer during the grinding process," *Proc. SPIE* **8415**, 84150K (2012).
9. I. K. Sung et al., "A swing arm method for profile measurement of large optical concave surfaces in the lapping process," *Int. J. Adv. Manuf. Technol.* **29**, 113–117 (2006).
10. L. Jia et al., "Principle and experiments of swing-arm profilometer," *Opt. Precis. Eng.* **15**(4), 499–504 (2007).
11. X. Luo, "Swing arm profilometer: improving the testing accuracy of large mirrors with shorter arms," *Chin. Opt. Lett.* **12**, S22202 (2014).
12. L. Xiong et al., "Measurement of 2m SiC aspheric mirror based on swing arm profilometer," *Acta Opt. Sin.* **35**(12), 1212002 (2015).
13. L. Xiong et al., "Swing arm profilometer: analytical solutions of misalignment errors for testing axisymmetric optics," *Opt. Eng.* **55**(7), 074108 (2016).
14. "Capacitive displacement sensors and systems," http://www.micro-epsilon.com/download/products/cat--capaNCDT--en.pdf.

**Ling Xiong** received her BS degree in optics from Northwestern Polytechnical University, in 2012. Currently, she is a PhD student at CIOMP (Changchun Institute of Optics, Fine Mechanics and Physics, Chinese Academy of Sciences). She is working on optical testing for large diameter optic segments. Her research interests include swing arm profilometer tests.

**Xiao Luo** received his BA degree in precision machinery and precision instrumentation in 2006 from the University of Science and Technology of China and a PhD in optical engineering in 2011 from CIOMP. He is an associate professor at CIOMP. His work includes fabrication with stressed lap and tests with swing arm profilometer for large aspherics. His interests also include hydraulic polishing support of large mirrors, MRF processing of large mirrors, and so on.

**Hai-xiang Hu** received his BS degree in physics from the University of Science and Technology of China, in 2012. Currently, he is a PhD student at CIOMP. His research interest includes high-efficiency processing and testing technology for large mirrors.

**Zhi-yu Zhang** received his BA and MS degrees from Jilin University of Technology and a PhD degree from Tohoku University. He is an associate professor of CIOMP. His research interest is set as optical fabrication by ultraprecision machining and laser direct writing. He has been working for more than 10 years on diamond turning of optics such as silicon, germanium, silicon carbide, aluminum, and aluminum-based composites.

**Feng Zhang** received his BS and MS degrees from Changchun University of Science and Technology and a PhD degree from CIOMP. He is a professor and PhD adviser at CIOMP. His research focuses on advanced technologies for optical fabrication.

**Li-gong Zheng** received his BA degree in mechanical design and manufacturing from Jilin University of Technology in 1992 and a PhD in optical engineering from CIOMP. He is a professor at CIOMP. His research focuses on advanced technologies for optical fabricating and testing.

**Xue-jun Zhang** received his BA degree from Jilin University of Technology, in 1992, MS and PhD degrees in CIOMP. He is a professor and PhD adviser at CIOMP, where he is also director of the Key Laboratory of Optical System Advanced Manufacturing Technology. His interest is advanced optical system manufacturing.